Astron. Astrophys. 330, 753–763 (1998)

ASTRONOMY AND ASTROPHYSICS

Origin and production of C(^{1}D) atoms in cometary comae

G.P. Tozzi[1], **P.D. Feldman**[2], **and M.C. Festou**[3]

[1] Osservatorio Astrofisico di Arcetri, Largo E. Fermi 5, I-50125 Firenze, Italy (tozzi@arcetri.astro.it)
[2] Department of Physics and Astronomy, The Johns Hopkins University, Baltimore, MD 21218, USA
[3] Observatoire Midi-Pyrénées, 14, avenue E. Belin, F-31400 Toulouse, France

Received 5 June 1997 / Accepted 15 September 1997

Abstract. The abundance of carbon atoms in the metastable ^{1}D state near the cometary nucleus provides an important diagnostic of one of the principal sources of carbon in the cometary coma. This quantity may be determined in two independent ways: measurement of ^{1}D–^{1}P fluorescence at 1931 Å and by prompt emission of the ^{1}D–^{3}P doublet at 9823/9850 Å. The latter is analogous to the [O I] $\lambda\lambda$6300/6364 emission that is often used to determine the cometary water production rate, but has not been extensively exploited to date. We have re-examined the C I λ1931 emission observed in some bright comets by the *International Ultraviolet Explorer*, and have compared these data to both the brighter resonance transitions, C I $\lambda\lambda$1657 and 1561, and the CO Fourth Positive band system when the latter are observed with sufficient signal-to-noise ratio. We find a strong correlation between the derived C(^{1}D) and CO production rates that suggests that photodissociation of CO is the primary source of the observed C(^{1}D) atoms in the coma. The photodissociation rate required by these data is significantly higher than the rates currently in the literature. Dissociative recombination of CO^+ is found to be only a minor source of C(^{1}D). In the future, ground-based observations of the 9823/9850 Å doublet at sufficiently high spectral resolution should provide a means for routinely determining the CO abundance relative to that of water in comets and how this ratio varies from comet to comet, with important implications to the physical aging of comets.

Key words: comets – ultraviolet: solar system – molecular processes

1. Introduction

It is only since spacecraft have visited the coma of comet 1P/Halley and investigated the properties of both its gaseous and solid phases that it has been determined that carbon is probably present in comets with solar abundance. Yet, the form in which carbon is stored in the volatile fraction of the nucleus remains an open question. The most direct way to determine the total carbon abundance is through ultraviolet spectroscopy of the emissions of C I and C II as, ultimately, all species are photodissociated or photoionized into their atomic constituents. Orbiting observatories such as the *International Ultraviolet Explorer* (*IUE*) or the *Hubble Space Telescope* (*HST*) sample only a small region of the central coma in which many carbon bearing species may deliver atoms so that the determination of the origin of carbon atoms in comae requires coupled information about many different species.

Possible production mechanisms of C(^{1}D) atoms are the photodissociation of neutral C-bearing species, the dissociative recombination of C-bearing ions and electron impact excitation of carbon and C-bearing molecules. As we shall see below, almost independent of coma chemistry, it is possible to show that the C(^{1}D) atoms come predominantly from a single source, CO. This is a key step towards a general discussion of the overall atomic carbon abundance in comets, a study that is deferred to a separate paper (Festou et al. 1997).

The ^{1}D state of carbon is metastable, with a lifetime of 4077 s (Hibbert et al. 1993). As a consequence, C(^{1}D) atoms can absorb sunlight before they decay to the ^{3}P ground state of atomic carbon and fluoresce in the ($2p^2\ ^1$D – $2p3s\ ^1$P^o) transition at 1931 Å (see Figure 1). This line was first observed in comet C/1975 V1 (West) by Feldman and Brune (1976) who also found that CO and C(^{3}P) were produced at roughly similar rates, suggesting that CO was the primary source of the atomic carbon observed in the coma. Photodissociation of CO_2 as a source of CO, and ultimately C, was considered on the basis that the CO_2^+ ($\tilde{B}\ ^2\Sigma_u\ -\ \tilde{X}\ ^2\Pi_g$) double band at 2884/2896 Å was detected and that this was an indication that the corresponding neutral molecule existed in the nucleus. This source, however, was believed to be insufficient because of the absence of CO Cameron bands that allowed an upper limit to the CO_2 production rate to be derived. CO_2 was not regarded as a likely candidate for carbon production since its main dissociation mode is into CO and O, and since the short-lived C(^{1}D) atoms would not be produced near the center of the coma as observed. CO as the sole parent of carbon atoms presented a difficulty in that its lifetime was rather long, as pointed out by A'Hearn and Feldman

Send offprint requests to: G.P. Tozzi

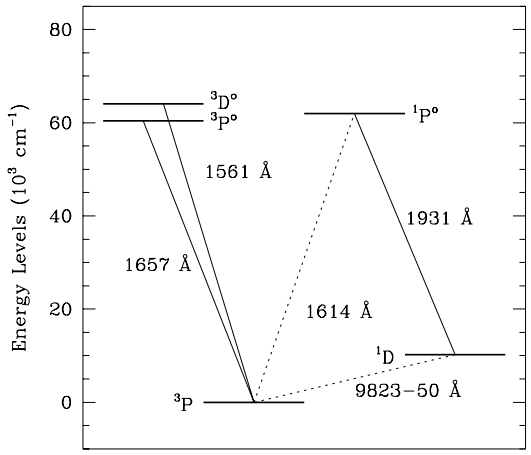

Fig. 1. Partial Grotrian diagram of atomic carbon showing the transitions of importance for this study. Full lines indicate allowed transitions; dashed lines are forbidden transitions.

(1980) from *IUE* observations of comet C/1979 Y1 (Bradfield), and confirmed by Festou (1984) from the study of a larger set of *IUE* observations. It thus appeared necessary to identify an additional carbon parent. Because of the high density of CO^+ inferred to be present from the strong CO^+ First Negative band emission observed in comet West, Feldman and Brune (1976) also suggested that electron recombination of CO^+ ions could be an efficient source of C(^{1}D) atoms.

With the many remote and *in situ* observations of comet 1P/Halley made in 1985–86, the problem of the abundance of carbon in comets became more complex. Not only did many new candidates appear as potential parents of carbon atoms in the coma but data accumulated that indicated that some parent species, including CO (see e.g., Krankowsky 1991; Eberhardt et al. 1987), could be produced from grains or other molecules in the extended coma itself. Many unknown species could reside in the gaseous as well as in the solid phases of the nucleus, making the resolution of the problem apparently intractable. As these new facts emerged, a large set of data on the ultraviolet emissions of CO molecules and C(^{3}P) and C(^{1}D) atoms has continued to accumulate, obtained since 1978 by the *IUE*. We note that emission from the Cameron bands of CO, principally due to prompt emission following the photodissociation of CO_2, was first reported in *HST* observations of comets 103P/Hartley 2 and C/1991 T2 (Shoemaker-Levy) by Weaver et al. (1994), and recently confirmed by the observation of the same emission in reprocessed *IUE* spectra (Feldman et al. 1997), thus allowing us to constrain the role of the CO_2 molecule in the carbon chemistry.

Our approach in this paper is to demonstrate that a correlation exists between the column densities of CO and C(^{1}D) atoms and that it is possible to account for the observed C(^{1}D) atoms from the direct photodissociation of CO. The effects of time-variability of the source, quenching of C(^{1}D) atoms by parent molecules, excess velocity of the atomic fragments and the extended source of CO are considered and shown to have only small influence on our conclusions. This conclusion is supported by the analysis of Feldman et al. (1997) that showed significant variation in the ratio of CO and H_2O production rates amongst comets and by the lack of suitable other carbon-bearing molecules to serve as a direct source of C(^{1}D) atoms.

2. Data analysis

2.1. Selection of data

IUE data from the short wavelength prime (SWP) spectrograph in the 1400–2000 Å range show emission features of C I, S I and CO (Feldman, 1982) and no solar continuum, except for some grating scattered light from longer wavelengths (Feldman 1986a). The *IUE* database contains about one hundred long exposure SWP spectra of comets that were taken between 1978 and 1992, i.e., well exposed spectra for which exposure times are $\geq$ 2700 s. Whereas the C(^{3}P) emissions are at times quite strong, the emissions from CO and C(^{1}D) are always weak so that the number of useful exposures is limited. Even amongst the long exposures, less than half reveal the presence of C I λ1931 or CO emissions. Since the exciting solar flux is low at wavelengths below 2000 Å, detection of CO with *IUE* requires a comet both with a water production rate of order or in excess of 10^{29} molecules s^{-1} and situated at a heliocentric distance of less than $\sim$ 1 AU. Table 1 lists all of the "on nucleus" spectra in which the C I λ1931 line is detected. Some of the spectra also show the presence of the CO Fourth Positive bands. Exposures with poor tracking accuracies were eliminated (see Festou 1990 for details on individual observations prior to 1990). Fourth Positive bands were observed in only 4 comets observed by *IUE*, all of which may be considered "moderately bright" comets. This can be partly understood as CO has a low fluorescence efficiency and the *IUE* SWP camera has low sensitivity near 1500 Å.

2.2. Data reduction

The presence of camera reseau marks very close to the C I multiplet at 1657 Å and the C I line at 1931 Å, the existence of noise spikes that can lie quite close to the expected emissions, and the fact that some emissions do not fill the slit while the standard *IUE* data processing integrates over the entire slit, makes the one dimensional spectra available from the ULDA (Uniform Low Dispersion Archive) archives unsuitable for our purposes. Instead, we used the flux calibrated extended line-by-line spectra (ELBL) available from the National Space Science Data Center Data Archive and Distribution Service (NSSDC-DADS). A spatial integration was made over the central rectangular portion of the large aperture (14 lines, each 1.″07 wide, almost perpendicular to the dispersion direction that do not include any reseau mark). The resulting one-dimensional spectra have been converted to surface brightness (in rayleighs) averaged over the $9.''07 \times 15.''3$ slit. Two examples, one from comet Bradfield and the other from 1P/Halley, are shown in Fig. 2a. We have also examined SWP comet spectra now available from the *IUE* final archive that have been recently reprocessed with the *NEWSIPS*

Table 1. "On-nucleus" *IUE* SWP long exposures in which the C I λ1931 emission is present: geometry of observations and derived average brightnesses in a 9.″07 × 15.″3 aperture.

SWP N°	Comet	Date dd-mm-yy	r (AU)	$\dot{r}$ (km/s)	Δ (AU)	Exposure time (s)	CO 1509 Å (R)	C I 1931 Å (R)
03025	C/1978 T1 (Seargent)	18-10-78	0.925	+33.9	0.76	10800	< 36	19 ± 5
07625	C/1979 Y1 (Bradfield)	10-01-80	0.712	+24.0	0.62	7200	48 ± 12	81 ± 9
07630	C/1979 Y1 (Bradfield)	11-01-80	0.719	+24.3	0.60	3600	< 66	53 ± 7
07668	C/1979 Y1 (Bradfield)	16-01-80	0.798	+26.3	0.41	3600	< 51	24 ± 7
07757	C/1979 Y1 (Bradfield)	24-01-80	0.919	+27.8	0.20	7200	< 48	16 ± 5
27422	1P/Halley	30-12-85	1.029	−26.6	1.13	11700	45 ± 12	36 ± 9
27884	1P/Halley	09-03-86	0.839	+24.7	1.07	2700	150 ± 30	109 ± 10
27898	1P/Halley	11-03-86	0.867	+25.2	1.02	7200	76 ± 21	67 ± 9
27906	1P/Halley	12-03-86	0.886	+25.5	1.00	3600	< 255	85 ± 22
27908	1P/Halley	13-03-86	0.901	+25.6	0.96	4200	85 ± 21	61 ± 7
27914	1P/Halley	15-03-86	0.919	+25.8	0.94	2460	< 135	70 ± 10
27927	1P/Halley	16-03-86	0.945	+26.1	0.89	5400	117 ± 28	50 ± 9
27945	1P/Halley	18-03-86	0.972	+26.3	0.84	11400	61 ± 13	29 ± 5
37722	C/1989 Q1 (Okazaki-Levy-Rudenko)							
		02-12-89	0.77	+19.5	0.52	4800	< 50	34 ± 8
38739	C/1989 X1 (Austin)	07-05-90	0.79	+35.3	0.45	5400	< 42	20 ± 5
38750	C/1989 X1 (Austin)	09-05-90	0.83	+35.1	0.42	11700	21 ± 6	24 ± 4
39538	C/1990 K1 (Levy)	26-08-90	1.38	−20.3	0.43	8400	38 ± 12	17 ± 5
39656	C/1990 K1 (Levy)	18-09-90	1.13	−16.0	0.84	14400	47 ± 14	30 ± 5
39658	C/1990 K1 (Levy)	18-09-90	1.13	−16.0	0.84	14400	43 ± 14	38 ± 5
46279	109P/Swift-Tuttle	15-11-92	1.062	−12.2	1.20	8100	< 45	20 ± 4
46320	109P/Swift-Tuttle	23-11-92	1.01	−9.4	1.27	2700	< 90	27 ± 5

software. These have somewhat better S/N ratio but are also afflicted with the same variable background found in the ELBL spectra. They give almost identical results for the extracted spectra.

Since some of the CO bands are blended with C I transitions, extraction of CO and C I intensities was made through a multiple linear fit to the C I and CO features together with a polynomial background. In the fitting procedure, we imposed a fixed FWHM (9.5 Å) to all of the lines (the width of the CO bands at rotational temperatures $\leq$ 200 K is $\leq$1 Å), and set the relative intensity of all the CO bands according to the fluorescence efficiencies computed below. In addition, CO band wavelengths were not allowed to change. Since these bands are sometimes blended with stronger atomic lines, the fitting procedure would have failed in identifying and determining the strength of these components. The spectra extracted by this technique are shown in Fig. 2b. The residual spectra, i.e., observed minus calculated, shows only noise and this assures that no spectroscopic features have been overlooked in the analysis. This also provides an estimate of the statistical uncertainty in these derived values. An uncertainty of 10% was added to account for the absolute calibration uncertainties. When a line is undetectable over the noise, we assume an upper limit three times the standard deviation measured in the residual spectrum over the line width.

In addition, small sources of systematic error may be present. Since only a few strong CO features are unblended, these lines are consequently "driving" the CO fit. Roettger (1991) suggested that the derived CO column density may in some comets be large enough that the strongest bands connecting with the ground vibrational level may be saturated, although this is dependent on the CO rotational temperature, T_{rot}, adopted. We have examined this possibility for the strong (1,0) and (2,0) bands by computing the absorption equivalent widths for these bands assuming that the relative populations of the rotational levels are given by T_{rot} = 200 K and that the widths of the individual lines are characterized by a velocity dispersion dominated by the gas outflow which we represent by a Gaussian of 1.6 km s^{-1} width. Of course, a complete analysis of this problem would require spectrally resolving the rotational structure, which is not possible in this case. At a CO column density of 1×10^{14} cm^{-2} the deviation from optically thin fluorescence is $< 10\%$ and reaches $\sim 25\%$ at 5×10^{14} cm^{-2}. From the discussion in Sect. 4.2 below, we find that the maximum derived CO column density (averaged over the aperture) is $\sim 5 \times 10^{14}$ cm^{-2}, so that we can conclude that saturation effects in these two bands are small and treat the CO emission as optically thin fluorescence. In all cases then, the (1,0) band brightness given in Table 1 is the brightness of that band that gives the best overall fit to the optically thin synthetic spectrum. We have also neglected the possible contribution of the S I λ1478 multiplet that has been shown to be significant only at relatively small heliocentric velocities (Roettger et al. 1989). Another source of error

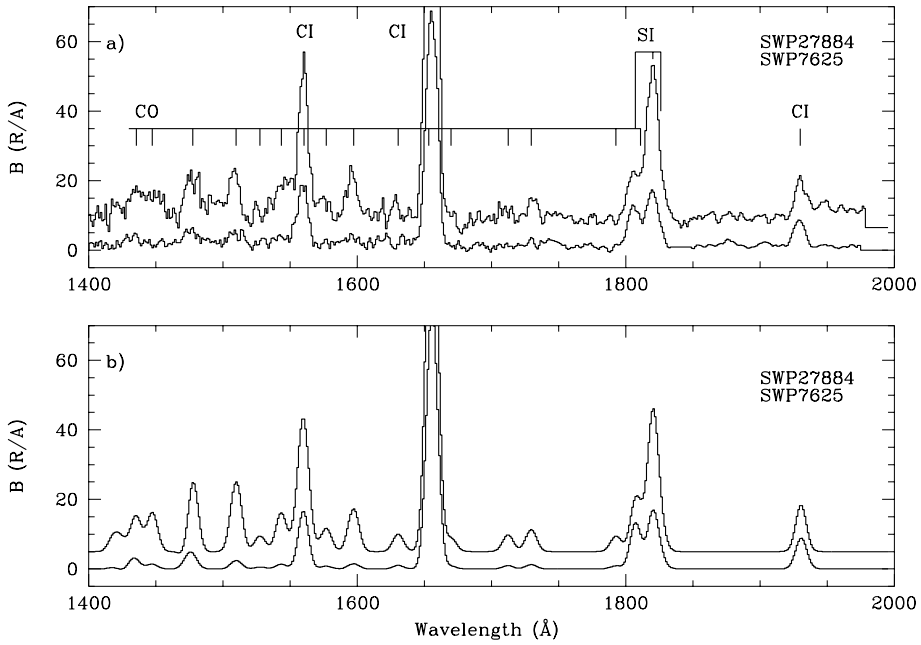

Fig. 2. a *IUE* spectra of comets Bradfield (SWP 7625) and 1P/Halley (SWP 27884). The spectrum of Halley has been shifted upward for clarity by 10 R/Å. Only CO, C I and S I transitions are detected. **b** Synthetic spectra produced using the procedure described in the text.

may be our assumption that the CO bands are produced only by radiative scattering, neglecting any possible electronic excitation. While the radiative transfer problem is considerably more complex, we justify our approach and choice of parameters by the rather good fit of the data to the optically thin synthetic spectra and by the good agreement of the derived CO production rate for 1P/Halley at the time of the *Giotto* encounter to that derived from the *in situ* measurements.

3. Fluorescence efficiencies

For all of the C I lines we re-computed the fluorescence efficiencies (g-factors) as a function of heliocentric velocity assuming the oscillator strengths from the recent compilations of Morton (1991) and Hibbert et al. (1993). No particular care was necessary for the ($2p^2\ ^1$D – $2p3s\ ^1$P^o) C I line at 1930.9 Å because its lower state is single and the solar spectrum is almost without structure over this region and shows only slight variation ($\sim$4%) with solar activity. The computed g-factor at 1 AU is 1.33×10^{-4} photons atom^{-1} s^{-1}. For the other two C I multiplets, at 1561 Å ($2p^2\ ^3$P – $2s2p^3\ ^3$D^o) and 1657 Å ($2p^2\ ^3$P – $2p3s\ ^3$P^o), it is necessary to know the relative population of the fine structure ground configuration. Moreover, the solar spectrum is very structured showing the same carbon lines in emission, self-absorbed, whose intensity depends on solar activity. This structure gives rise to a "Swings' effect", or variation of the g-factor with heliocentric velocity of the comet. The high resolution solar spectrum used for multiplet g-factor computation is taken from the Ultraviolet Spectrometer and Polarimeter of the *Solar Maximum Mission* (Tandberg-Hanssen et al. 1981). This is a disk center spectrum which we take to be representative of the whole disk under quiet sun conditions. To determine the whole disk flux, this spectrum has been convolved and scaled to match a low resolution flux-calibrated *UARS/SOLSTICE* spectrum (Woods et al. 1993) that was obtained at a time of low solar activity in March 1995. The change with solar activity is taken into account using data from the *Solar Mesosphere Explorer* satellite, which monitored the solar ultraviolet flux from 1981 to 1988. The results of these calculations, which will be discussed in detail by Festou et al. (1997), show that the values of the g-factors, at 1 AU, varied from 0.02×10^{-4} to 0.14×10^{-4} photons s^{-1} atom^{-1} for the 1561 Å multiplet and from 0.24×10^{-4} to 0.5×10^{-4} photons s^{-1} atom^{-1} for the other multiplet at 1657 Å.

As already mentioned, the column density of CO was derived from the brightness of the CO Fourth Positive bands assuming radiative scattering without an electron excitation contribution. While previous studies of CO abundance in comets used the values of fluorescence efficiency from Durrance (1981), scaled to the appropriate heliocentric distance and with rough estimates of the variation from solar minimum to solar maximum (Feldman, 1986b; Woods et al., 1986), the availability of more recent solar flux data cited above led us to re-evaluate the g-factors for the Fourth Positive bands for the optically thin case. The absorption oscillator strengths were taken from the recent compilation of Morton and Noreau (1994) and the branching ratios are from Kurucz (1976). The same solar flux data were used as above. As with the earlier published values, with the exception of the (0,v'') and (5,v'') bands, the CO g-factors show very little dependence on heliocentric velocity or rotational temperature (Feldman et al. 1976) and are assumed to be independent of those parameters. However, the g-factors are uniformly lower than those of Durrance, implying in general higher relative CO abundances than previously reported. The variation with solar activity has been evaluated using the solar flux data from the *Solar Mesosphere Explorer* satellite and found to be relatively small, of the order of 20% for the continuum which is responsible for almost all of the CO absorption. Fortuitously,

Table 2. CO Fourth Positive system fluorescence efficiencies appropriate for low solar activity, a rotational temperature of 200 K, and zero heliocentric velocity.

Transition (v', v'')	Band Head (Å)	g-factor (10^{-7} ph s^{-1} atom^{-1})
5 0	1392.6	0.36
4 0	1419.1	0.38
5 1	1435.4	0.62
3 0	1447.4	1.13
4 1	1463.6	0.28
2 0	1477.6	1.77
3 1	1493.7	0.15
1 0	1509.9	1.92
4 2	1510.4	0.055
2 1	1525.9	0.043
5 3	1527.7	0.22
3 2	1542.5	0.47
0 0	1544.5	0.52
4 3	1559.7	0.13
1 1	1560.4	1.00
2 2	1576.9	0.50
0 1	1597.3	0.93
4 4	1611.5	0.080
5 5	1629.1	0.18
2 3	1630.6	0.42
3 4	1648.1	0.26
0 2	1653.2	0.77
1 3	1670.1	0.38
3 5	1705.4	0.15
0 3	1712.4	0.40
4 6	1724.1	0.093
1 4	1729.6	0.65
5 7	1743.3	0.057
2 5	1747.5	0.17
0 4	1775.2	0.14
1 5	1792.8	0.45
2 6	1811.2	0.31

the g-factors for solar minimum are very close to those used by Woods et al. (1986) in the analysis of long-slit ultraviolet spectra of P/Halley, who had taken the values from Durrance, for solar maximum, and reduced them by a factor of two for solar minimum. Table 2 gives the computed CO g-factors at r = 1 AU.

Morton and Noreau (1994) have pointed out that the CO ($d\,^3\Delta_i$ – $X\,^1\Sigma^+$) (5,0) band perturbs the strong (1,0) Fourth Positive band ($A\,^1\Pi$ – $X\,^1\Sigma^+$) at 1510 Å and so has an appreciable f-value for absorption. However, since the transition is spin forbidden, all of the (5,v'') transition probabilities in the spectral region of the Fourth Positive system are very small (the $d\,^3\Delta_i$ state decays primarily to $a\,^3\Pi$) and fluorescence from this system does not alter appreciably our calculated g-factors.

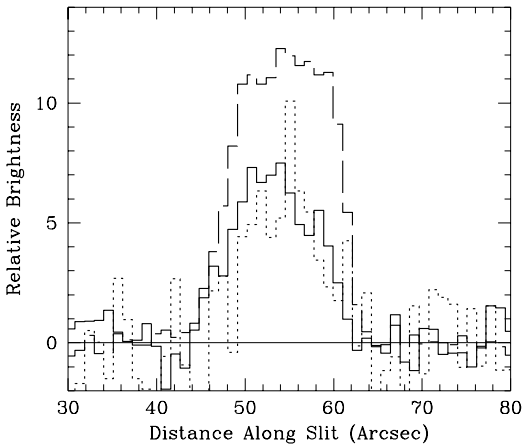

Fig. 3. Brightness variation along the long axis of the *IUE* aperture in a well tracked short wavelength spectrum (SWP 27884) of the C I λ1931 line in 1P/Halley (solid line). For comparison the profiles of the C I λ1657 (long dashed line) emission and the strongest bands of the CO Fourth Positive system (dotted line) are also shown. Despite a low SNR, the CO brightness profile suggests that the emission is peaked in the inner coma.

4. Results and discussion

4.1. Spatial profiles

For a comet at a geocentric distance, Δ, of 1 AU, the projected $9\farcs07 \times 15\farcs3$ central rectangular region of the *IUE* aperture at the comet is 6600×11000 km^2. This linear size is comparable to the C(^{1}D) scale length due to the short lifetime of C(^{1}D) atoms (4077 s) and implies that the spatial distribution should be close to that of its parent species. Limited spatial resolution ($\sim 5''$) perpendicular to the dispersion can be extracted from *IUE* spectra, an example being given in Fig. 3. Despite the low signal-to-noise ratio, the C I λ1931 emission appears narrower than that of C I λ1657, which appears nearly flat over the central $15''$ of the aperture. This is as expected since a parent distribution would vary approximately as the inverse of the cometocentric distance. In addition, the C I λ1931 and CO Fourth Positive profiles also appear similar. Further spatial information is available from long off-nucleus exposures, typically taken when the comet is centered in the long wavelength large aperture so that the projected distance is ~48000 km for a comet at Δ = 1 AU. Although the C I λ1657 emission is seen, C I λ1931 is never detected. Again, this is the expected behavior if C(^{1}D) atoms are produced through the direct photodissociation of a species directly residing in the nucleus. The effect of an extended source of CO on the observed C I λ1931 emission will be discussed in Sect. 5.3 below.

4.2. Column abundances

Table 3 gives the C(^{1}D) and CO column densities derived for the optically thin case using the fluorescence g-factors calculated above. Only spectra in which the SNR of the C I λ1931 emission is > 3 have been used to derive the C(^{1}D) atom abun-

Table 3. Column densities (model-independent) and CO production rates (model-dependent) derived from *IUE* "on-nucleus" SWP long exposures.

SWP N°	Comet	$\overline{N}(^3\mathrm{P})$ (10^{12} cm^{-2})	$\overline{N}(^1\mathrm{D})$ (10^{12} cm^{-2})	$\overline{N}(^3\mathrm{P})/\overline{N}(^1\mathrm{D})$	$\overline{N}$(CO) (10^{12}cm^{-2})	Q(CO) (10^{27}s^{-1})	Q_d(CO) (10^{27}s^{-1})	Q(H$_2$O) (10^{28}s^{-1})	Q_d(CO)/Q(H$_2$O)
03025	C/1978 T1	3.1 ± 0.3	0.12 ± 0.03	25.3	< 130	< 7.9	7.9 ± 2.2	25.5	0.031 ± 0.009
07625	C/1979 Y1	7.9 ± 0.8	0.31 ± 0.05	25.7	100 ± 25	5.1 ± 1.3	12.8 ± 1.9	14.6	0.088 ± 0.013
07630	C/1979 Y1	7.7 ± 0.8	0.21 ± 0.03	37.3	< 140	< 7.0	8.7 ± 1.1	14.6	0.060 ± 0.008
07668	C/1979 Y1	3.8 ± 0.4	0.12 ± 0.04	33.0	< 140	< 4.5	4.0 ± 1.5	10.9	0.045 ± 0.014
07757	C/1979 Y1	2.0 ± 0.2	0.10 ± 0.03	20.1	< 170	< 4.2	4.3 ± 1.4	5.70	0.075 ± 0.025
27422	1P/Halley	11.7 ± 1.2	0.29 ± 0.07	41.0	250 ± 70	22.8 ± 6.0	33.3 ± 8.1	41.5	0.080 ± 0.020
27884	1P/Halley	23.0 ± 2.4	0.58 ± 0.08	39.9	560 ± 110	48.4 ± 9.7	49.7 ± 6.7	75.0	0.066 ± 0.009
27898	1P/Halley	17.4 ± 1.7	0.38 ± 0.06	45.7	300 ± 90	25.0 ± 7.0	33.3 ± 5.6	58.4	0.057 ± 0.010
27906	1P/Halley	18.6 ± 1.9	0.50 ± 0.14	37.0	< 1060	< 86.4	45.8 ± 12.7	69.1	0.066 ± 0.018
27908	1P/Halley	18.3 ± 1.8	0.37 ± 0.06	50.2	360 ± 90	28.1 ± 6.9	33.6 ± 5.1	59.8	0.056 ± 0.009
27914	1P/Halley	18.8 ± 1.9	0.44 ± 0.08	42.5	< 600	< 45.6	41.1 ± 7.2	47.1	0.087 ± 0.015
27927	1P/Halley	14.8 ± 1.5	0.34 ± 0.07	43.6	560 ± 130	40.0 ± 9.4	31.9 ± 6.6	49.0	0.065 ± 0.013
27945	1P/Halley	14.5 ± 1.5	0.20 ± 0.04	71.0	300 ± 60	20.4 ± 4.2	19.5 ± 3.9	49.2	0.040 ± 0.008
37722	C/1989 Q1	3.6 ± 0.4	0.15 ± 0.04	24.2	< 120	< 5.2	6.7 ± 1.7	4.16[a]	0.101 ± 0.024
38739	C/1989 X1	3.3 ± 0.4	0.09 ± 0.03	35.6	< 110	< 3.6	4.1 ± 1.1	10.2	0.025 ± 0.006
38750	C/1989 X1	2.9 ± 0.3	0.12 ± 0.02	23.5	60 ± 19	1.7 ± 0.5	5.6 ± 1.1	10.2	0.034 ± 0.004
39538	C/1990 K1	5.8 ± 0.8	0.24 ± 0.08	24.0	300 ± 100	10.1 ± 3.3	22.5 ± 7.0	20.1	0.112 ± 0.035
39656	C/1990 K1	8.0 ± 0.8	0.29 ± 0.06	28.0	250 ± 70	16.8 ± 4.9	25.2 ± 4.9	20.1	0.125 ± 0.024
39658	C/1990 K1	10.2 ± 1.0	0.36 ± 0.06	28.0	230 ± 70	15.4 ± 4.9	32.2 ± 5.3	20.1	0.160 ± 0.026
46279	109P	10.6 ± 1.1	0.17 ± 0.04	62.8	< 230	< 22.3	20.8 ± 4.6	29.1	0.071 ± 0.016
46320	109P	12.8 ± 1.3	0.21 ± 0.04	62.2	< 420	< 43.0	24.6 ± 5.2	50.5	0.049 ± 0.010

[a] Extrapolated from an observation at r = 1.041 AU assuming an r^{-3} dependence.

dances. Also included in the table are the C(^{3}P) column densities from Festou et al. (1997). The values of C(^{3}P) column density span over an order of magnitude, up to 2×10^{13} cm^{-2}, where the C I $\lambda\lambda$1561 and 1657 transitions may, under certain conditions, saturate. However, Festou et al. (1997) have demonstrated, through several different lines of argument, that the emissions are produced by radiative scattering and that they remain optically thin so that the emission brightness is a reliable measure of the average column density in the field of view. We note from the table that a close relationship appears between the $\overline{N}(^1\mathrm{D})$ and $\overline{N}(^3\mathrm{P})$ column densities that can be expressed as $\overline{N}(^3\mathrm{P}) = 40 \pm 12\,\overline{N}(^1\mathrm{D})$, which, independent of any model, shows us that the two quantities are directly proportional and probably genetically related. The relationship between the column densities of C(^{1}D) and CO is not as obvious, and this is the consequence of the CO photodissociation rates being dependent on heliocentric distance and solar activity, as discussed in the following section.

4.3. CO photodestruction rates

The column densities derived above allow us to directly assess the rates of photodestruction of CO in a cometary coma. We consider only the three primary channels:

$$\begin{aligned} \mathrm{CO} + \mathrm{h}\nu &\rightarrow \mathrm{C}(^3\mathrm{P}) + \mathrm{O}(^3\mathrm{P}) && (a)\\ &\rightarrow \mathrm{C}(^1\mathrm{D}) + \mathrm{O}(^1\mathrm{D}) && (b)\\ &\rightarrow \mathrm{CO}^+ + \mathrm{e} && (c) \end{aligned}$$

with rates $J_d(^3\mathrm{P})$, $J_d(^1\mathrm{D})$, and J_i, respectively. Then, assuming that CO is vaporized directly from the nucleus (the effect of an extended source will be discussed below), since the lifetime of C(^{1}D) is much shorter than that of CO, the ratio of the observed column density of C(^{1}D) to CO in the *IUE* slit should be less than (or equal) to the equivalent ratio of the total number N_t of particles in the coma, *i.e.*,

$$\frac{\overline{N}(^1\mathrm{D})}{\overline{N}(\mathrm{CO})} \leq \frac{N_t(^1\mathrm{D})}{N_t(\mathrm{CO})} = \frac{Q(^1\mathrm{D})\tau(^1\mathrm{D})}{Q(\mathrm{CO})r^2\tau(\mathrm{CO})} \qquad (1)$$

where $\tau(^1\mathrm{D})$ is equal to 4077 s, independent of the heliocentric distance, r, and τ(CO) is evaluated at 1 AU. The photodissociation rate into C(^{1}D) at 1 AU, $J_d(^1\mathrm{D})$, is by definition:

$$J_d(^1\mathrm{D}) = \frac{Q(^1\mathrm{D})}{Q(\mathrm{CO})\tau(\mathrm{CO})} \geq \frac{\overline{N}(^1\mathrm{D})}{\overline{N}(\mathrm{CO})\tau(^1\mathrm{D})/r^2} \qquad (2)$$

In Fig. 4 the right-hand term of this equation is plotted as a function of the geocentric distance, for the comets listed in Table 1 with measurable CO Fourth positive band emission. From the figure we can derive limits for the photodissociation rate to C(^{1}D) of $\geq 1.5 \times 10^{-7}$ and $\geq 3.5 \times 10^{-7}$ s^{-1} for quiet and active sun conditions, respectively. It is important to note that these values are derived assuming only CO as parent with a point like source and that they do not depend on any model. These values are about a factor of 3 higher than those given in the compilation of solar photodestruction rates of Huebner et al.

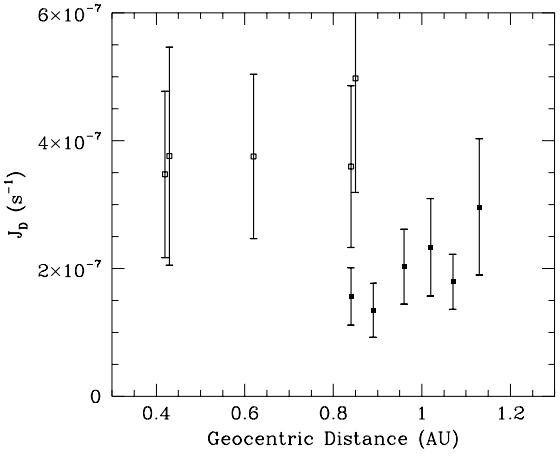

Fig. 4. Lower limits for the CO photodissociation rate to C(^{1}D) vs the geocentric distance. Full and open squares are for quiet and active sun conditions, respectively.

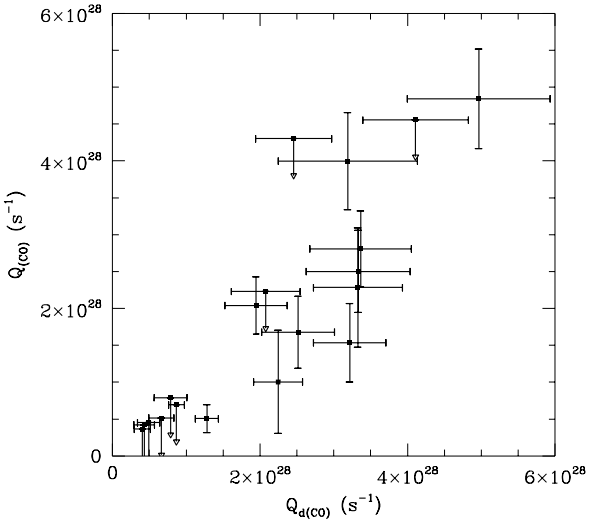

Fig. 5. Relation of CO production rates derived from Fourth Positive band system measurements (Q(CO)) compared with those derived from the C I λ1931 line (Q_d(CO)). Values and upper limits are in excellent agreement, considering the generally low S/N ratio of the data.

(1992). Since the scale length for C(^{1}D) decay is comparable to the dimensions of the *IUE* slit projected onto the comet, it is likely that these limits are within a factor of two or three of the actual values.

A model is necessary to determine the C(^{1}D) column density if we want to obtain J_d (^{1}D) and not just an upper limit, since a fraction of the C(^{1}D) atoms decay outside of the *IUE* field of view. The vectorial model (Festou 1981) was used assuming a CO outflow velocity of $0.85r^{-0.5}$ km s^{-1}. For excess velocity of dissociation of the daughter species there is some uncertainty. Huebner et al. (1992) give as excess energy 2.56 and 2.29 eV, corresponding to $\sim$ 4.9 and $\sim$ 3.9 km s^{-1}, for C(^{3}P) and C(^{1}D), respectively. These velocities depend mainly on the wavelength of the strong solar lines relative to the dissociation thresholds. Assuming that predissociation at wavelengths shortward of 1200 Å is the most efficient channel for CO dissociation and taking into account the coincidence of solar ultraviolet emissions (Wilhelm 1992) with the predissociating bands (Eidelsberg and Rostas 1990) we have re-evaluated the excess velocity to be of the order of 4 km s^{-1} for C(^{3}P). Since for C(^{1}D) it is more difficult to compute the excess velocity, we assumed it to lie between 3.9 km s^{-1}, the value given by Huebner et al., and 1 km s^{-1}, the mean outflow velocity in the collision zone. We will consider both possible cases in the discussion below.

Since CO Fourth Positive emission is well measured only in ten *IUE* spectra, six of them being of 1P/Halley, we must keep in mind that the presence of the distributed source of CO at $\sim 10^4$ km from the nucleus (Eberhardt et al. 1987) and the variability of the production rate (Feldman et al. 1987) may introduce some errors. However, as we discuss below, the uncertainty is less than 25% for the observations made with the *IUE* slit.

The results for J_d(^{1}D) give a quasi-unique solution almost independent of the total CO photodestruction rate. The values for the quiet sun are $(3.7 \pm 1.0) \times 10^{-7}$ s^{-1} with v_d = 1 km s^{-1} and $(8 \pm 2) \times 10^{-7}$ s^{-1} with v_d = 3.9 km s^{-1}. For the active sun we have five spectra, one each of Bradfield (C/1979 Y1) and Austin (C/1989 X1) and three of Levy (C/1990 K1). Unfortunately, the spectra of comet Levy may have a strong blend at 1931 Å due to the (2,0) Cameron band (Feldman et al. 1997). The values that we obtain are about 40% higher than that obtained for quiet sun conditions.

A check on the hypothesis that CO is the main parent of C(^{1}D) may be made by computing the CO production rate from C(^{1}D) column densities, Q_d(CO), for all of the spectra where we have only an upper limit to the brightness of the CO Fourth Positive System and good S/N ($\geq$ 3) for the C I λ1931 line. In this case we assumed v_d = 3.9 km s^{-1} and the corresponding J_d. These values may be compared with the upper limits to Q(CO) derived from the upper limit to the CO column density, both of which are listed in Table 3 and shown in Fig. 5. Almost all of these values are in agreement, with a few exceptions.

Our analysis excludes other possible carbon-bearing parent molecules, such as methanol, found to have an abundance of $\sim$ 5% with respect to water in some comets (Crovisier 1994) since they cannot dissociate directly but require multiple steps to produce atomic carbon. These would not give C I λ1931 with the emission profile seen in Fig. 3.

The last column of Table 3 gives the production rate of CO, computed from the C(^{1}D) column density, with respect to that of water. For Q(H_2O) we have re-evaluated *IUE* long wavelength measurements of OH emission at 3085 Å, taken as close in time as possible to the SWP observations, using the formalism of Budzien et al. (1994) to evaluate the H_2O and OH lifetimes as a function of solar activity. Where there is overlap, for the observations of 1P/Halley, these results are in accord with the recent analysis of Combi et al. (1993) of data from the same source. We note that for the post-perihelion Halley observations, the ratio Q(CO)/Q(H_2O) is typically 6–8%, slightly higher than the value of 4% for the component of CO vaporized directly

from the nucleus given by Eberhardt et al. (1987) from *Giotto* NMS measurements. However, as discussed in Sect. 5.3 below, the *IUE* aperture will include a contribution from the distributed source of CO described by Eberhardt et al., so that are results are in good agreement with the *in situ* measurements of relative CO abundance (see also the discussion in Feldman et al. 1997). Note also, for Bradfield, that the ratio Q(CO)/Q(H_2O) is about a factor of two higher than that given previously by Feldman (1986b). The difference is accounted for by the different g-factors used and the fact that the earlier result was based on only a single measured band, not on a fit to the entire spectrum.

The smallest values of $J_d(^1\mathrm{D})$ that we obtain (with v_d = 1 km s^{-1}) from the data are about an order of magnitude higher than those given by Huebner et al. (1992), 3.47×10^{-8} and 7.87×10^{-8} s^{-1}, for quiet and active sun, respectively. If we make the hypothesis that the ratio $J_d(^1\mathrm{D})/J_d(^3\mathrm{P})$ given by Huebner et al. is close to the correct value, then, by inference, we would expect $J_d(^3\mathrm{P})$ to be about 10 times higher than that of Huebner et al. as well. With these rates, photodissociation dominates photoionization as the principal channel of CO photodestruction. Therefore, the total lifetime of CO would be considerably shorter than the value given by Huebner et al. This is in agreement with long slit spectrograph observations of comet C/1989 X1 (Austin), where, to explain the observed profile of C I λ1657, a short CO lifetime, equal to 4×10^5 s, corresponding to a $J_t(^3\mathrm{P})$ of 2.5×10^{-6} s^{-1} (solar maximum), is needed (Sahnow et al. 1993). A similar conclusion was reached by Woods et al. (1987) regarding long-slit spectra of 1P/Halley.

Huebner et al. used relatively low resolution CO absorption cross sections in evaluating CO photodissociation rates. More recent higher resolution data that include predissociating channels through a number of high-lying states of the CO molecule were used by Fox and Black (1989) to re-evaluate the total dissociation rates in connection with a study of the thermosphere of Venus. They found values for $J_d(^3\mathrm{P}+\ ^1\mathrm{D})$ of 4.4×10^{-7} and 1.21×10^{-6} s^{-1}, for quiet and active conditions, respectively, compared with 3.16×10^{-7} and 7.39×10^{-7} s^{-1}, given by Huebner et al., about a factor of 1.5 higher. Unfortunately, the pathways to C(^{1}D) through these additional channels are not clear and a similar calculation of $J_d(^1\mathrm{D})$ was not done.

However, in view of these new results, it is likely that the excess velocity of C(^{1}D) is lower than that used and/or that the dissociation branching to the ^{1}D is higher than the 10% value quoted by Huebner et al. We note that a different excess velocity would also change the results of Sahnow et al. (1993). Another possibility is that solar wind electrons play an important role in the dissociation of CO, as suggested recently by Bhardwaj et al. (1996). However, their analysis suggests significant electron impact excitation of features such as C I λ1329 and C II λ1335 that are not seen in the *IUE* spectra, and that the role of electrons is confined to regions of the coma inside 1000 km from the nucleus which will affect only slightly the total emission seen in the *IUE* aperture. Moreover, the measured ratios of the C I λ1657 to λ1561 brightness are very close to the values predicted for radiative scattering (Festou et al. 1997).

In the future, observations that measure all the emission of C I λ 1931 or the near IR decay lines (see Section 6) would be independent of the ^{1}D excess velocity, and thus give a more reliable evaluation of the CO production rate.

5. Other C(^{1}D) production and loss mechanisms

Here we briefly discuss the other possible mechanisms that may increase or reduce the population of the carbon in the metastable ^{1}D level.

5.1. Dissociative recombination

One of the first processes proposed after the discovery of the C I λ1931 emission in comet West was dissociative recombination of CO^+ (Feldman 1978). According to Huebner et al. (1992), the CO photoionization rate is comparable to that for photodissociation (see above) so that CO^+ ions are formed abundantly and accelerated into the ion tail. However, in the inner coma, these ions can recombine with electrons into dissociating molecular states leading to the production of C(^{1}D) atoms. Feldman (1978) estimated that dissociative recombination would be efficient in producing C(^{1}D) in a region just outside the collision zone. At smaller cometocentric distances collisions between carbon and water will quench the C(^{1}D), while at larger distances the electron and ion densities are too low. However, the density of free electrons is strongly dependent on the solar flux, is peaked in the inner coma, and is a function of Q_{H_2O} (Ashihara 1978). Consequently, if dissociative recombination were the dominant source of C(^{1}D), a steep dependence (r^{-4}) of the ratio $\overline{N}(^1\mathrm{D})/\overline{N}(^3\mathrm{P})$ with heliocentric distance should be present in the data. This is not the case as can be seen from Table 3, where the ratio does not show a clear dependence on r. Moreover, the fact that C(^{1}D) has been detected in comets such as Bradfield with very little CO^+ is an indication that the contribution of this mechanism must be small.

5.2. The effect of collisions

For a comet close to the sun and with a large gas production rate there are collisional processes that may change the relative population of C(^{1}D) atoms and these can be very efficient in the inner coma. In particular, because of the long radiative lifetime of the ^{1}D level (4077 s), the collision of neutral molecules, particularly water, with the atoms can reduce considerably the population of this level. The inverse process, i.e., excitation from the ground state to the ^{1}D level is negligible because of the low kinetic energy of the molecules with respect to the energy of the ^{1}D level. Only energetic electrons produced by the photoionization of water (Ashihara 1978) can contribute efficiently to populate the metastable level, but only in a comet with a very high gas production rate and very close to the sun.

To evaluate the importance of these two processes and referring to Fig. 1, we consider only two levels of carbon: ^{3}P and ^{1}D. We neglect solar radiative excitation to the $^1\mathrm{P}^o$ level because this level decays back quickly, producing the 1931 Å

line, with negligible effect on the ^{1}D population. The possible electronic excitation and de-excitation rates, C_{12} and C_{21}, together with that of de-excitation (quenching) produced by water, C_{H_2O}, have to be compared with the rate for spontaneous decay, A(^{1}D) = 2.45 $\times$ 10^{-4} s^{-1}. The only difference is that the excitation rate has to be multiplied by the local density of carbon atoms in the ^{3}P state, while the de-excitation rate by the density of ^{1}D atoms.

From the vectorial model (Festou 1981), assuming CO as a parent with a branching ratio ^{1}D:^{3}P equal to 10:90, we estimate the density ratio of $n(^3\mathrm{P})$ to $n(^1\mathrm{D})$ to be of the order of 16 for cometocentric distances smaller than 10^3 km. The excitation coefficient for electronic impact depends on the electron energy, but its maximum value is $\approx 7\times10^{-8}$ cm^{-3} s^{-1} (Pequignot and Aldovrandi 1976). The value of n_e can be deduced from Ashihara (1978) who computed a flux of electrons produced by water photoionization, with energies in the range 2–12 eV, of 3×10^8 electrons eV^{-1} cm^{-2} s^{-1} sr^{-1}, at a cometocentric distance of 500 km for a comet with $Q_{H_2O} = 10^{30}$ molecules s^{-1} at r = 1 AU. This flux corresponds to a density n_e of the order of 100 cm^{-3}. Since the electron flux, and hence the density, is proportional to r^{-2} (solar flux) and Q_{H_2O} (water density) we find for a typical Halley observation with r = 0.9 AU and $Q_{H_2O} = 7 \times 10^{29}$ molecules s^{-1}, the electron density is $\approx$80 cm^{-3}. This gives a maximum value of the excitation rate $C_{12} \approx 6 \times 10^{-6}$ s^{-1}. Taking into account that this has to be multiplied by the density of carbon in the ground ^{3}P state, electron collisions increase the population of the ^{1}D level by a maximum of 34% at a cometocentric distance ρ = 500 km. Even if at shorter distances this contribution is larger, the variation in the column density averaged over the *IUE* slit is negligible with respect to our measurement errors.

The contribution of the electron impact to de-excitation is much smaller because the de-excitation rate C_{21} should be of the same order of magnitude as C_{12} (the photoelectrons are more energetic than the energy of the ^{1}D level and the ratio of the statistical weights of the two considered levels is within a factor 2), but to compute the transition rate the excitation rate has to be multiplied by the carbon density in the ^{1}D level, i.e. a value about 16 times lower than that for ^{3}P. We thus conclude that for the spectra considered here the variation of column densities within the *IUE* slit produced by electron collisions is negligible. However, it can be important in the inner coma and it may possibly be detected in spectra obtained with higher spatial resolution, as for example with *HST*.

On the other hand, collisional quenching by water is more important because of the larger density of water molecules relative to electrons, even if the rate coefficient for such collisions is low, about 1.7 $\times$ 10^{-11} cm^{-3} s^{-1} (Schofield 1979). Assuming radial outflow of the water, at relatively small cometocentric distances the water density is proportional to its production rate (Q_{H_2O}), to the inverse of the water outflow velocity (V_{H_2O}) and the the square of the cometocentric distance (ρ). For a typical Halley spectrum with $Q_{H_2O} = 7\times10^{29}$ molecules s^{-1} and V_{H_2O} = 0.9 km s^{-1}, the computed density at ρ = 10^3 km is equal to 6.2 $\times$ 10^7 cm^{-3}. The quenching rate is then 1 $\times$ 10^{-3} s^{-1}, i.e. four times faster than the radiative decay. However, this quenching produces only a decrease of 18% in the observed intensity of the C I λ1931 line when integrated over the *IUE* slit. This conclusion is also supported by the C I λ1931 profile shown in Fig. 3, which does not show strong evidence of quenching close to the nucleus for the observation of Halley with the highest H_2O production rate.

5.3. Extended source

The presence of an extended source contributing to the CO production rate two-thirds of the total, and peaked at about 10^4 km from the nucleus, was detected in Halley by the *Giotto* neutral mass spectrometer (Eberhardt et al. 1987). Even if for the spectra considered here the peak of the extended source lies outside the *IUE* slit, this source will contribute to the observed column density and must be taken into account. To evaluate the effect produced by the extended source we used the vectorial model in order to reproduce the CO density profile of Eberhardt et al. As expected the intensity profile shows an increase in the region close to 10^4 km, but a much smaller relative contribution at shorter distances. Fig. 6 shows an unperturbed profile together with that computed taking account of quenching by water and with an extended source for a typical observation of Halley. The increase of the column density averaged over the *IUE* slit is only 9%.

Excitation by electron impact is not included in the figure because it affects the profile only at distances shorter than about 500 km. From the figure we can see that spatially resolved observations of C I λ1931 (or of the near infrared transitions downward from C(^{1}D), described below) with good spatial resolution can disentangle the three effects that we have considered: electron impact, water collisions, and the CO distributed source. The last possibility is particularly significant in that it would allow us to determine if a distributed source of CO is a common characteristic of all comets.

6. Infrared emissions

As shown in Fig. 1, the metastable level ^{1}D can spontaneously decay to the ground state emitting two lines at 9823.4 and 9849.5 Å (air wavelengths). The photon intensity ratio of these near-infrared lines to the ultraviolet fluorescence at 1931 Å depends only on the solar flux, atomic parameters and the heliocentric distance r, and is equal to

$$\frac{I([\mathrm{CI}]\ \lambda\lambda 9823/9850)}{I(\mathrm{CI}\ \lambda 1931)} = \frac{A(^1\mathrm{D})}{g_{1931}/r^2} \qquad (3)$$

where $A(^1\mathrm{D})$ is the transition probability for spontaneous decay and g_{1931} is the g-factor at r = 1 AU. The numerical values are: g_{1931} = 1.33 $\times$ 10^{-4} s^{-1} at 1 AU; $A(^1\mathrm{D})$ is 1.8 $\times$ 10^{-4} s^{-1} and 0.6 $\times$ 10^{-4} s^{-1} for the ^{1}D– ^{3}P$_2$ (9850 Å) and ^{1}D– ^{3}P$_1$ (9823 Å) lines, respectively (Hibbert et al. 1993). The brightness (in rayleighs) of the stronger infrared line is then of the same order of magnitude as C I λ1931 at r = 1 AU, and is three

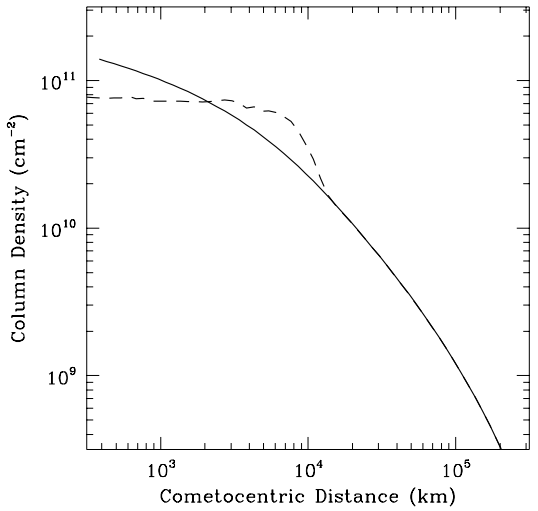

Fig. 6. Simulation of the spatial distribution of CO column density for a typical observation of P/Halley with an extended source and water quenching. The solid line is for a comet without quenching or an extended source while the dashed line is the simulation for Halley with $Q_{H_2O} = 7 \times 10^{29}$ molecules s^{-1} and an extended source of CO based on the *in situ* observation of Eberhardt et al. (1987).

times higher at a heliocentric distance of 1.5 AU. However, the intrinsic brightness of these IR lines decreases with heliocentric distance, because of the decrease in CO production rate and of the CO photodissociation rate.

A search for the near-infrared lines in comet 109P/Swift-Tuttle was not successful because of blends with OH lines present because of the moderate spectral resolution available (FWHM = 5 Å) (Tozzi et al. 1994). However, we estimate that a resolution of $\approx$ 1 Å is sufficient to separate the two lines from the nearby OH emissions and to reduce the signal of continuum due to dust scattering. While [C I] $\lambda\lambda$9823/9850 are detected in other sources such as planetary nebulae (Liu et al. 1995), to our knowledge only once has one of these lines, the brighter one at 9850 Å, been detected in a comet. Using a narrow band Fabry-Perot interferometer (FWHM $\approx$ 0.4 Å), Münch et al. (1986) reported a preliminary value of 8 ± 1 rayleighs of [C I] λ9850 within a $2'$ field-of-view in observations of 1P/Halley made on December 14 and 22, 1985 (r = 1.29 and 1.16 AU for the two dates, respectively). By scaling this value to the *IUE* slit we get an expected brightness of 55 R for this line from which Eq. 3 predicts 24 and 30 R for C I λ1931, again for the two dates. This may be only an upper limit if the distributed source of CO was present in December 1985 as this source is more important in the field-of-view of the Fabry-Perot than in the small field-of-view of the *IUE*. Unfortunately, there are no *IUE* measurements on the exact dates given above. Nearest in time are data from December 30, 1985, when the C I λ1931 brightness measured by *IUE* was 36 ± 9 R (see Table 1), in agreement with the predicted value, taking into account the smaller heliocentric distance of the comet at the later date.

7. Conclusion and summary

The production of carbon atoms in the ^{1}D metastable state in a cometary coma has been re-examined using the archive of cometary *IUE* spectra. It has been shown that the most probable mechanism of its production is photodissociation of CO. Other possible mechanisms for the production and loss of C(^{1}D) and the effect of a possible distributed source have been examined and they have been found to produce small effects for *IUE* measurements, but can be important for observations made with a smaller field-of-view, such as with *HST*. C(^{1}D) is thus a tracer of CO and can be used to determine the production rate of CO, even when CO fluorescence is undetectable. Since C(^{1}D) can be measured from the ground by means of the two near-infrared lines produced by radiative decay, future spatially resolved observations can be expected to elucidate the degree of quenching of C(^{1}D) by water, the contribution of electron impact excitation, and the possible presence of an extended source of CO in other comets. Such observations are an important complement to ground based measurements at radio wavelengths successfully used during the last few years to observe CO in comets (see *e.g.* Biver et al. 1997). While the radio observations are more sensitive to CO in distant comets, they lack in spatial resolving power (only recently, the technique of radio interferometry, which can give good spatial and spectral resolution, has been attempted for comets Hyakutake (C/1996 B2) and Hale-Bopp (C/1995 O1)), while the technique discussed here is capable of providing important information on the spatial distribution of CO in the coma.

The value of the photodissociation rate to the ^{1}D state required by the *IUE* observations is about one order of magnitude larger than that computed by Huebner et al. (1992). This implies that either the branching ratio for dissociation to ^{1}D is much higher than the $\approx$10% value given by these authors or that the total photodissociation rate of CO is considerably larger than their calculated value. Fox and Black (1989) have shown, using more complete spectroscopic data on CO, that inclusion of predissociation from high-lying states of CO can increase the total photodissociation rate by about a factor of 1.5 over that computed by Huebner et al., but a similar calculation for C(^{1}D) has not been performed. A similar need for a higher photodissociation rate was derived from long slit measurements of C I λ1657 emission in comet Austin (Sahnow et al. 1993). Since electron impact dissociation does not appear to be sufficient to account for the difference, this discrepancy remains an open question.

Acknowledgements. Most of the spectra used in this analysis were supplied by the NASA NSSDC (National Space Science Data Center Data Archive and Distribution Service). GPT and PDF thank the Johns Hopkins University and the Arcetri Observatory, respectively, for supporting their mutual visits. This research was partially funded by the Italian Council of Research, National Astronomical Group (CNR-GNA). MCF acknowledges the support from the *Action Thématique Planétologie* from the *Centre National de la Recherche Scientifique* (Paris). The work at the Johns Hopkins University was supported by NASA grant NAG5-2141.

References

A'Hearn, M. F., Feldman, P. D. 1980, ApJ 242, L187
Ashihara, O. 1978, Icarus 35, 369
Bhardwaj, A., Haider, S. A., Singhal, R. P. 1996, Icarus, 120, 412
Biver, N., Bockelée-Morvan, D., Colom, P., et al. 1997, Science 275, 1915
Budzien, S. A., Festou, M. C., Feldman, P. D. 1994, Icarus 107, 164
Combi, M. R., Bos, B. J., Smyth, W. H. 1993, ApJ 408, 668
Crovisier, J. 1994, in *Asteroids, Comets, Meteors 1993*, edited by A. Milani, M. DiMartino and A. Cellino (Kluwer, Dordrecht, 1994), 313
Durrance, S. T. 1981, J. Geophys. Res. 86, 9115
Eidelsberg, M., Rostas, F. 1990, A&A 235, 472
Eberhardt, P., Krankowsky, D., Schulte, W., Dolder, U., Lämmerzahl, P., Berthelier, J. J., Woveries, J., Stubbermann, U., Hodges, R. R., Hoffman, J. H., Illiano, J. M. 1988, A&A 187, 481
Feldman, P. D. 1978, A&A 70, 547
Feldman, P. D. 1982, in *Comets*, edited by L. L. Wilkening (The University of Arizona Press, Tucson, AZ), 461
Feldman, P. D. 1983, Science 219, 347
Feldman, P. D. 1986a, A&A 159, 342
Feldman, P. D. 1986b, in *Asteroids, Comets and Meteors II*, ed. C.-I. Lagerkvist, B. A. Lindblad, H. Lundstedt & H. Rickman, Uppsala Univ., Uppsala, 1986, 263
Feldman, P. D., Brune, W. H. 1976, ApJ 209, L45
Feldman, P. D., Festou M. C., A'Hearn M. F., Arpigny C., Butterworth P. S., Cosmovici C. B., Danks A. C., Gilmozzi R., Jackson W. M., McFadden L. A., Patriarchi P., Schleicher D. G., Tozzi G. P., Wallis M. K., Weaver H. A., Woods T.N. 1987, A&A 187, 325
Feldman, P. D., Festou, M. C., Tozzi G. P., Weaver H. A. 1997, ApJ, 475, 829
Feldman, P. D., Opal, C. B., Meier, R. R., Nicolas, K. R. 1976, in *The Study of Comets*, NASA SP-393, 773
Festou, M. C. 1981, A&A 95, 69
Festou, M. C. 1984, Adv. Space Res. 4, 9, 165
Festou, M. C., 1990, IUE–ULDA Access Guide, Wamsteker, W. Ed., N°2, *Comets*, ESA SP-1134
Festou, M. C., Feldman, P. D., Tozzi, G. P. 1997, in preparation
Fox, J. L., Black, J. H. 1989, GRL 16, 291
Hibbert, A., Biémont, E., Godefroid, M., Vacek, N. 1993, A&AS 99, 174
Huebner, W. F., Keady, J. J., and Lyon, S. P., 1992, Adv. Space Sc., 195, 1
Krankowsky, D., 1991, in *Comets in the Post-Halley Era*, R. L. Newburn et al. Eds, Kluwer, vol. 2, 855.
Kurucz, R. L. 1976, SAO Special Report 374
Liu, X.-W., Barlow, M. J., Danziger, I. J., Clegg, R. E. S. 1995, MNRAS 273, 47
Morton, D. C. 1991, ApJS 77, 119
Morton, D. C., Noreau L. 1994, ApJS 95, 301
Münch, G., Hippelein, H., Hessmann, F., Gredel, R. 1986, International Halley Watch Spectroscopy Discipline hotline report (unpublished)
Pequignot, D. , Aldovrandi, S. M. V. 1976, A&A, 50, 141
Roettger, E. E. 1991, Comparison of Cometary Comae using Ultraviolet Spectroscopy: Composition and Variation. PhD Dissertation, The Johns Hopkins University, Baltimore, MD
Roettger, E. E., Feldman, P. D., A'Hearn, M. F., Festou, M. C., McFadden, L. A., Gilmozzi, R. 1989, Icarus, 80, 303
Sahnow, D. J., Feldman, P. D., McCandliss, S. R., Martinez, M. E. 1993, Icarus 101, 71.
Schofield, K. 1979, J. Phys. Chem. Ref. Data 8, 723
Tandberg-Hanssen, E. et al. 1981, ApJ 244, L127
Tozzi, G. P., Feldman, P. D., Weaver, H. A. 1994, A&A 285, L9
Wilhelm, K. (ed) 1992, The Sumer Spectrometer for SOHO - Solar Ultraviolet Measurements of Emitted Radiation. SUM-MPAE-RO-113000-02-00
Weaver, H. A., Feldman, P. D., McPhate, J. B., A'Hearn, M. F., Arpigny, C., Smith, T. E. 1994, ApJ 422, 374
Woods, T. N., Feldman, P. D., Dymond, K., Sahnow, D. 1986, Nature 324, 436
Woods, T. N., Feldman, P. D., Dymond, K. 1987, A&A 187, 380
Woods, T. N., Rottman, G. J., Ucker, G. J. 1993, JGR 98, 10679

This article was processed by the author using Springer-Verlag LaTeX A&A style file *L-AA* version 3.